

Review of the Manuscript:

Title: Shifting momentum balance and frictional adjustment observed over the inner-shelf during a storm

Written by M. Grifoll , A. Aretxabaleta , J. L. Pelegrí , and M. Espino

Manuscript No.:os-2015-23

General comments

Authors investigated the momentum balance in the Catalan (inner) shelf area of the NW Mediterranean Sea during the passage of storms. They explored this by, for the most part, analyzing current - meter observations at three locations in that shelf area. They offer an explanation about different responses of the shelf sea to the passage of storms. They show a very solid understanding of the balance of terms in the momentum equation in the along-shelf direction and one observes from the references that they are experienced in the circulation issues of that area linked to processes in the lower frequency domain with periods of a few days or longer. The paper reveals some possibly new findings and is also educative.

The English is quite solid. However, their explanation of different responses of the shelf relies on the incapacity of the bottom stress to dissipate high kinetic energy during the second storm, because there was a kinetic energy 'left-over' from the first storm. This is to be reflected on significant rapid oscillations with periods longer than 12 h of local acceleration and advective terms. In their abstract and in the manuscript they also point out that the response of the inner shelf (24 m depth) is 'prevailing frictional one'. One seems hardly to go together with the other: the 'prevailing frictional response' that is obviously not sufficient to dissipate the 'rapid' oscillations of local acceleration and advection terms. If however, one statement goes easily together with the other, then this deserves special attention in Discussion.

R2.1. We agree with the reviewer that there was confusion with the use of the term "prevailing frictional system" with the oscillations observed in the advection and acceleration terms. We called it "prevailing frictional response" to differentiate from the "inertial response" that prevails with increasing depth. However, your comment is highly appropriate and the new version of the manuscript has been modified to avoid the misunderstanding. We have removed the mentioned sentence from the abstract and we have modified the discussion addressing this point (see below). However, during the first phase of the storm there is a correspondence between the increase in wind stress, the acceleration and the bottom friction that is worth mention. The second phase of the storm, started with significant along-shelf velocities and sea level removing from the previous peak and the ocean response increase in terms of complexity.

Paragraph modified in the discussion:

"We may finally compare the cross-shelf changes of the frictional and geostrophic terms in the along-shelf momentum balance (Figure 9). Their relative importance can be explored by comparing the bottom frictional time (Equation 8) with the inertial time ($f^{-1} = 18.15$ h). During the peak of the storm (surface stress $\tau = 0.25$ Pa), the frictional and inertial times are equal for water depths of 94 m; for the average stress of the storm (surface stress $\tau = 0.12$ Pa) this happens for water depths of 64

m. Thus, the frictional effects dominated for depths up to around 60 m, causing our current meters to be located in regions controlled by inner-shelf dynamics during the whole storm. For the frictional and inertial times to be the same, the wind stress would have to be 0.075 Pa at 50 m and 0.02 Pa at 24 m. Therefore, the Coriolis term is relatively not important at 24 m except for very low surface stresses, such as during the calm period between the two storm pulses (0.02 Pa); during those times other terms, like the pressure gradient force, will dominate the along-shelf momentum balance (Grifoll et al, 2013).”

What is most certainly missing in the paper is a conception of how the two storms are really similar which is certainly reflected in the balance of terms in the momentum. Authors did not offer a single statement about that. Storms should be observed from the point of their extension, their travelling speeds, horizontal gradients of winds and air-pressure during the storm. Authors did attempt to capture the barotropic pressure gradients through the differences in pressures between the A2 station and the remote tidal gauge 64 km away. However, the reader misses the ‘image’ of both storms that pass over the Catalan shelf. It is true that ‘global atmospheric models’ (e.g. ECMWF) may still present difficulties revealing storms in their ‘true’ time and space scales. Nonetheless, even so one would get an image about the ‘similarity’ of the two storms -especially from the point of view of horizontal gradients of wind (and pressure) which most certainly influence the horizontal gradients of currents, and therefore advection terms which are extracted from the space difference of Eulerian measurements of velocity. This is the first key point missing from the paper: an estimate of horizontal gradients within the storm, i.e. if the first storm was horizontally much more ‘homogeneous’, then horizontal gradients of currents (and their depth average) in forced motion would be weaker, advective terms would be smaller, and ‘the non-sufficient friction’ explanation would not be sufficient...

R2.2. The extension of the storm may be inferred from atmospheric Sea Level Pressure. In the new version of the manuscript, we have included a new figure showing the sequence of the wind field and sea level pressure from Era-Interim reanalysis from ECMWF products (see new Figure 2 in the new version of the manuscript). This figure provides evidence that the model horizontal gradients are relatively smooth, and the low-pressure system is displacing gradually from the South to the North. Complementing this figure, the paragraph shown below has been modified in the new version of the manuscript addressing this reviewer comment.

Paragraph included in Section 2 “Site location, data and methods”:

“Additionally, synoptic information for the storm (winds and sea level pressure) was obtained from the ERA-Interim global reanalysis product by the European Centre for Medium Range Weather Forecasting (ECMWF).”

Paragraph added in Section 3.1

“We focus on the 12-15 March 2011 period, which includes the passing of a NE storm with maximum wind velocity of 13 m s^{-1} . The storm arose from the detachment of a low-pressure center from the Jet Stream between 11 and 12 March 2011, which reached the Iberian Peninsula (Figure 2). The low pressure remained centered over the Iberian Peninsula on 13 and 14 March, and by 15 March it weakened considerably. In our region, it was characterized by two energetic northeasterly wind peaks of similar magnitude (12 March 05:00 UTC and 14 March 15:00 UTC). A relatively

calm period in between the peaks lasting 22 hours with a slight reverse in wind direction (Figure 3.a) was caused by the low-pressure center being located over the study area. The storm finished on 15 March when the wind intensity decreased to zero.”

Additional Figure included (Figure 2 in the new version of the manuscript):

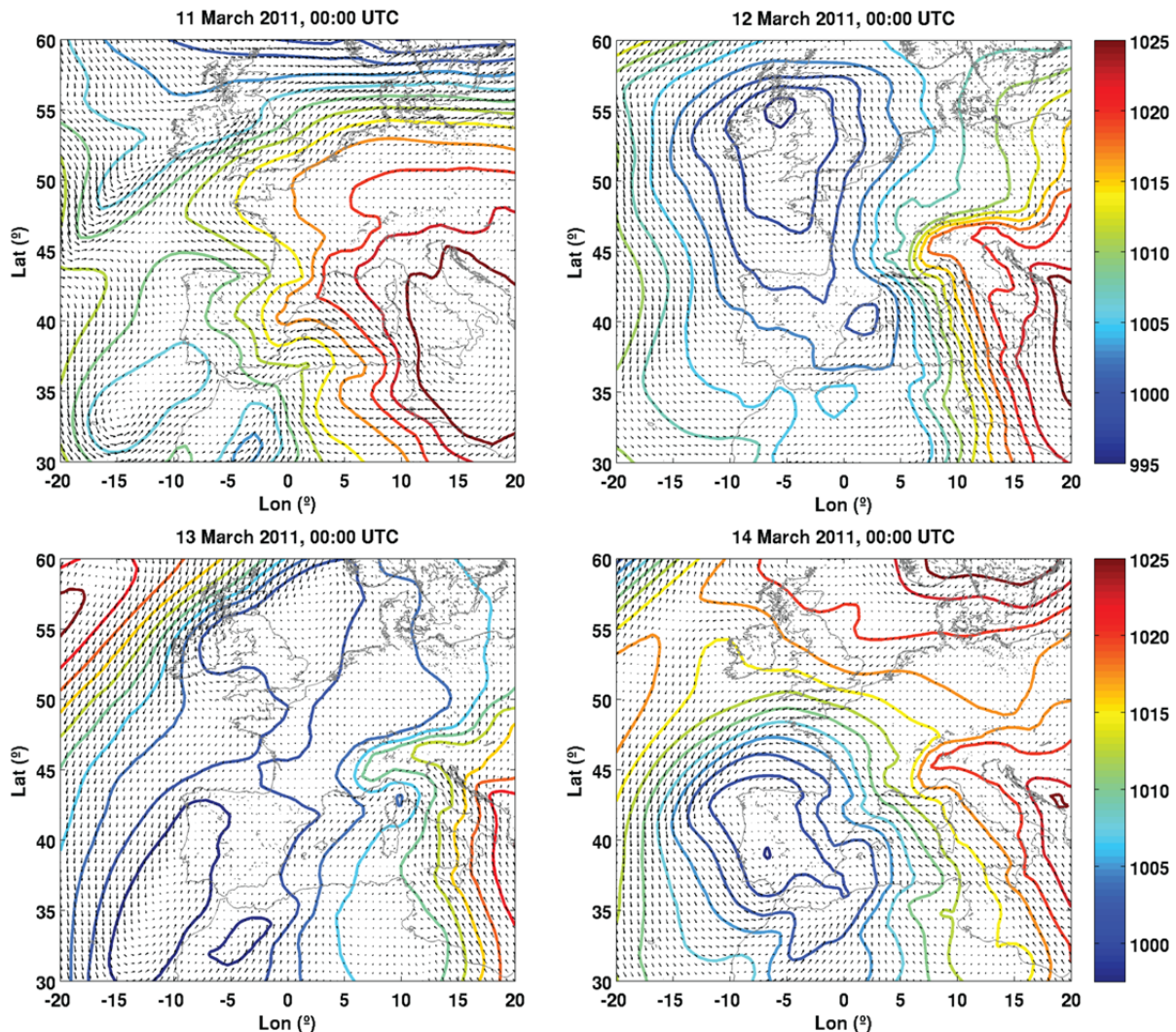


Figure 2. Regional charts of the mean sea level pressure (HPa) and winds for the sequence 11 – 14 March 2011. Data source: ERA-Interim global reanalysis from ECMWF.

A second key point missing from an otherwise well written paper is linked to the possibility of generating different long coastal waves by the passage of a storm. It is true that during a storm the current field would follow the wind field (and the air-pressure field), meaning a forced system. To know the time and space extension of this, one needs to have a look at the synoptic meteorological evolution of the storm mentioned earlier. After the cessation of the first storm and before the second storm passes over the shelf area, there are also free long waves on the shelf there is no word about them in the manuscript. Authors correctly inferred without any notion of long waves that if the second storm starts ‘early enough’ this means that the friction damping of motion raised by the first storm was not sufficient. However, it is the friction dissipation of free waves that matters here. Therefore during the second storm, if it arrives ‘early enough’ (say within 18 h after the first storm), there is a superposition of remaining long free waves from the first storm

with the forcing motion of the second storm...

What authors explored is the (in)significance of wind-driven surface waves, which could also be remotely generated (swell), with a period around 8 s on the balance of terms in the equation of motion. Returning to the concept of 'missing long shelf waves', questions arise: Are they trapped (or arrested in an offshore direction) topographic barotropic waves on a sloping bottom, present during and after the storm passage? Is the oscillation of local acceleration and advection terms also linked to inertial, or just-above inertial frequency phenomena?

Thanks for your comment. Responding also to the first reviewer comment, we have modified the discussion addressing this point. After a careful analysis of the data and referencing the basic literature (e.g. Gill, Csanady, Brink, etc.), we agree with the potential presence of transient and coastally trapped waves. Additional wavelets plots have been included (Figure 6 and 8) and the discussion has been modified accordingly (see section 4.1). This new approach is included in the manuscript (abstract, results, discussion, conclusions and an additional appendix) with a mention of the link between the oscillations in the momentum terms and in the water current velocity structure. See new appendix included at the end of the present document. In our opinion, your comment has enhanced notably the scientific quality of the paper.

Modifications in the discussion (Section 4.1. "Momentum evolution in the inner-shelf"):

"The along-shelf momentum balance during the second wind peak shares some characteristics with the first one. The acceleration term and the PGFR were enhanced during the increase in wind stress, reaching a maximum about 6 hours after the wind intensity peak. The along-shelf velocity decreased after the wind maximum. 12 hours into the calm period, the velocity exhibited a number of fluctuations (Figures 3.b and 3.d) that are reflected by the acceleration, advective, bottom friction, Coriolis and PGFR terms (Figure 4). These oscillations are consistent with oscillations in the lowest part of the water column in the cross-shelf velocities (Figure 3.c), and could be explained as a transient coastal current response to the sudden enhanced wind stress in the form of inertio-gravity waves (Kundu et al., 1983; Tintoré et al., 1995). These waves are associated at near-inertial motions as a result of the flow adjustment to the coast. Another plausible explanation of these oscillations is the generation of internal waves dispersed from the surface (wind-mixed layer) to larger depths in the lee of the storm (Gill, 1984; Kundu and Thompson, 1985). The characterization of the internal waves would require more detailed information of the stratification in the water column before and after the storm jointly with additional observations in the cross-shelf direction (for instance, in the presumably mixed-layer near-shore). Additionally, internal waves might explain the baroclinic two-layer mode observed in the cross-shelf velocities (Figure 3.c). Internal wave propagation is usually described in areas outside the continental shelf, as the frictional forces tend to limit its effectiveness in shallower areas like the inner shelf. Discarding other potential mechanisms, like the propagation of fast coastal Kelvin waves (Csanady, 1982; Gill, 1982), is not possible because of the limited observations. The 14-15 March oscillations in the along-shelf velocity (Figures 3.b and 3.d) are consistent with the local moderate increase in energy in the 12-16 hours band in the wavelet analysis (Figure 6).

The spectral and wavelet analyses of the velocity also show fluctuations with a dominant periodicity of 1-2 days (Figure 6). We propose that these sub-inertial fluctuations may reflect the propagation of free coastal waves, generated further upstream during the first part of the storm, into the study area. Hence, during the second peak of the storm, the velocity field results from a superposition of free waves and derived oscillations of wind-forced local motions described above.

The propagation of topographic waves is briefly considered in Appendix B, where Csanady's

(1982) coastal strip model is used to assess the magnitude of the oscillations for a linear and frictionless coastal band. The theoretical lowest-mode topographic waves have a period of about 32 hours, which is similar to the dominant period as deduced from the spectral and wavelet analyses (Figure 6). These sub-inertial waves were likely generated at the shelf in some northern location where the winds reached peaked values. Their presence seems consistent with the observed sea-level oscillations (Figure 3.e), as large as 0.05 m on time scales of about 1-2 days, giving rise to velocities of about 0.5 m s^{-1} (Figure 3.c). Jordi et al., (2005) described the existence of topographic waves in the NW Mediterranean Sea. They characterized the south-westward propagation with a relevant importance in the low frequency water current variability. Due to our limited observations, additional measurements and numerical modelling efforts (e.g., Brink and Chapman, 1985) are needed to properly characterize the relevance of topographic waves during storms.

The differences between the observed and residual pressure gradient forces, PGFO and PGFR, may be interpreted as arising from the transient (fast) oscillatory flow or the northward translation of the storm (Figure 2). The PGFR are necessary to balance the flow yet they differ substantially from the pressure gradient as calculated from the A2 and Blanes sea level gauges (64 km apart). Hence, we may interpret the PGFR as composed of two contributions: a first one as a result of the direct response to wind forcing, and a second one that arises from the propagating storm. This idea is further reinforced by the fact that the PGFR and acceleration time series are very similar (Figures 4.a and 4.g). Our interpretation is that the acceleration is composed of a relatively smooth contribution, which would drive the flow in the absence of waves (as it occurs during the first wind event), and an oscillatory part associated with the transient inertio-gravity waves. To test this idea we have calculated the difference, PGFR - PGFO, and have computed the energy and wavelet spectra (Figure 8). We find that there is a major energy peak in the 1-2 day band (topographic waves) and a smaller one in the 12-16 hour band, which we interpret as the transient waves. However, the characterization of the link between observed transient oscillatory flow and topographic waves is limited by the lack of observations to properly separate the local and remote dynamic conditions.”

Please, see references included at the end of this document. In the abstract we state:

“Before, during and after the second wind pulse, there were velocity oscillations with periods around 12-16 hours likely associated with transient waves.”

In the “Conclusions and final remarks” we include:

“During the calm period between wind peaks, the pressure gradient force reverted with the flow remaining southwestward and also velocity oscillations. We interpret the pressure residual, and the accompanying oscillations, as associated with the presence of transient waves due to the sudden wind stress input. During the second wind peak, the local response of acceleration, bottom stress and pressure gradients reoccurred, but with the along-shelf flow being influenced by the sub-inertial topographic waves, with velocity amplitudes as large as 0.5 m s^{-1} . These waves remained active even when the second wind peak had ended.”

Additional Figures included:

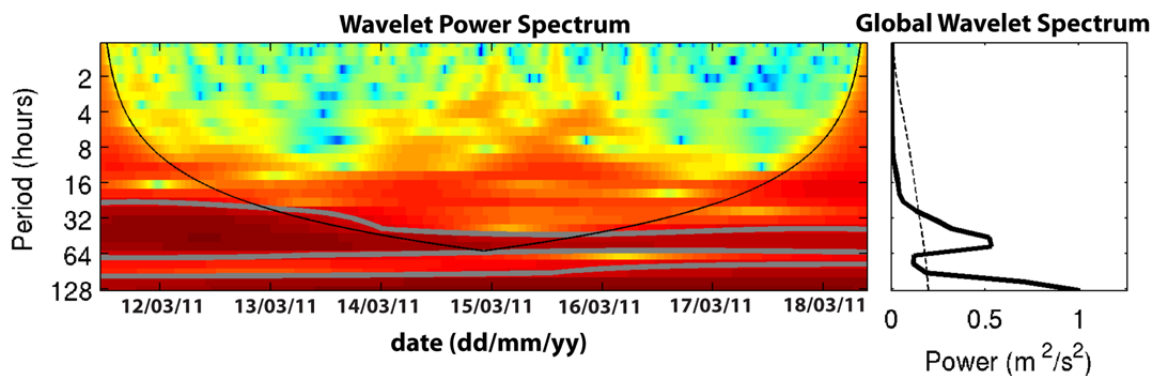


Figure 6. (Left) Wavelet analysis and (right) spectral analysis for the depth-averaged currents at station A2. The solid gray line in the wavelet diagram shows the energy values that exceed the significance level; similarly, the dashed line in the spectra diagram shows the significance level.

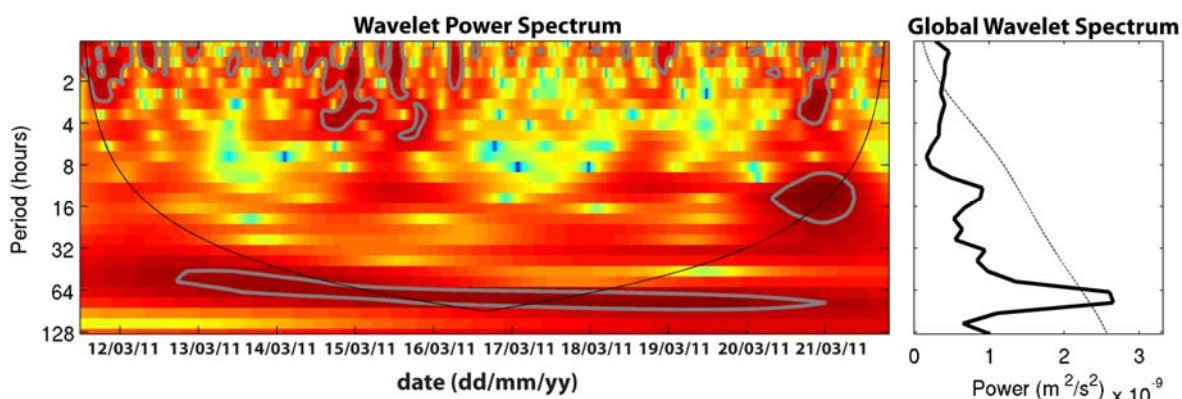


Figure 8. (Left) Wavelet analysis and (right) spectral analysis for the PGFR – PGFO. The solid gray line in the wavelet diagram shows the energy values that exceed the significance level; similarly, the dashed line in the spectra diagram shows the significance level.

During those storms was the radiation of internal waves from the surface (wind-mixed layer) to larger depths and horizontal distances also present, at least around the A2 station? This latter analysis requires knowledge of the stratification (before and after the storm), and authors did refer to it in a relatively modest sense by using CTD observations on 17th March 2011 for the estimate of thickness of the surface and bottom boundary layer. The spread of internal waves to depth may offer an explanation as to why at one place oscillations of acceleration of depth average currents are ‘not visible’ (or not pronounced) due to the baroclinic nature of motion (the first baroclinic two layer mode, visible on figure 2 c for the depth-time distribution of cross-shelf velocity), which after integration of currents along the vertical yield modest remaining depth averaged currents, which enter in vertically averaged equation of motion. This baroclinic nature of inertial motion during the passage of the storm was studied on flat bottom areas by Gill (JPO 1984, vol. 14, 1129-1151) and by Kundu and Thomson (JPO 1985, vol. 15, 1076-1084). Even if these issues cannot be resolved by pure analysis of currents at three locations, they deserve to be discussed and would make more sense in a context of the exploration of the balance of terms in the along-shelf (and across-shelf) direction. A plausible hypothesis of the existence of some long coastal waves with periods between 12 and 24 h generated during the storms, most likely topographic but also ‘flat-bottom long waves’, e.g. Kelvin and even Poincaré waves (angular frequency $\omega > f$, the Coriolis

parameter), could matter and certainly deserves attention.

A careful analysis of the data in A2 and A3 did not show a clear presence of inertial waves radiating away. Factors such as the accuracy of the devices, deficient information of the stratification in the water column or the complexity of the flow difficult the identification of internal wave from observations. However, this point is discussed in the new version of the manuscript because we agree that it deserves to be mentioned (see previous answer), jointly with the new wavelet plots (Figure 6 and 8 in the new version of the manuscript).

A third point is the careless introduction of the advective terms in the (long-shore) equation of motion (1). It is strange that authors did not pay any attention to the dynamics which can be ruled by the sloping bottom of the (inner) shelf (referring mostly to topographic waves). There are no horizontal gradients of the bottom depth in their analysis. This would be true if advective terms were not introduced. Authors derivation of terms in the Appendix is focused on the e-folding friction time scale (done correctly). The derivation of depth average of advective terms over a sloping bottom is not described. When these terms are introduced, however, some advective terms that apparently seem to be of the same order of local acceleration term, are missing in their key equation of motion (1). This might change their conclusions that the advective terms do not play a significant role in the(?) sense of transport, or depth averaged currents.

The advection related with the sloping bottom term is included in the analysis of the new version of the manuscript (see also the author's response in the following section). The conclusion does not differ significantly because the estimation of the size of the new non-linear term is still relatively small.

Modifications in the Manuscript:

“There are two additional momentum advection terms related to changes in the depth of the water column: $\frac{(\overline{uv})}{H} \frac{\partial H}{\partial x} - \frac{(\overline{v^2})}{H} \frac{\partial H}{\partial y}$. The first term, the cross-shelf slope term (CROS.SLP.), has to be retained in our analysis, while the second term is small, as the water depth is constant in the along-shelf direction.”

New Equation 1:

$$\underbrace{\frac{\partial \bar{v}}{\partial t}}_{\text{ACCE.}} + \underbrace{\frac{\partial \bar{v}^2}{\partial y}}_{\text{ADVEC.}} + \underbrace{\frac{\partial \overline{uv}}{\partial x}}_{\text{CROS.SLP.}} + \underbrace{\frac{(\overline{v^2})}{H} \frac{\partial H}{\partial y}}_{\text{COR.}} + f\bar{u} = -g \frac{\partial n}{\partial y} + \underbrace{\frac{\tau_{ys}}{\rho H}}_{\text{PRS.GRD.}} - \underbrace{\frac{\tau_{yb}}{\rho H}}_{\text{W.STR.}} - \underbrace{\frac{1}{\rho H} \left(\frac{\partial S_{yy}}{\partial y} + \frac{\partial S_{xy}}{\partial x} \right)}_{\text{B.STR. RAD.STR.}}$$

Figure 4 modified:

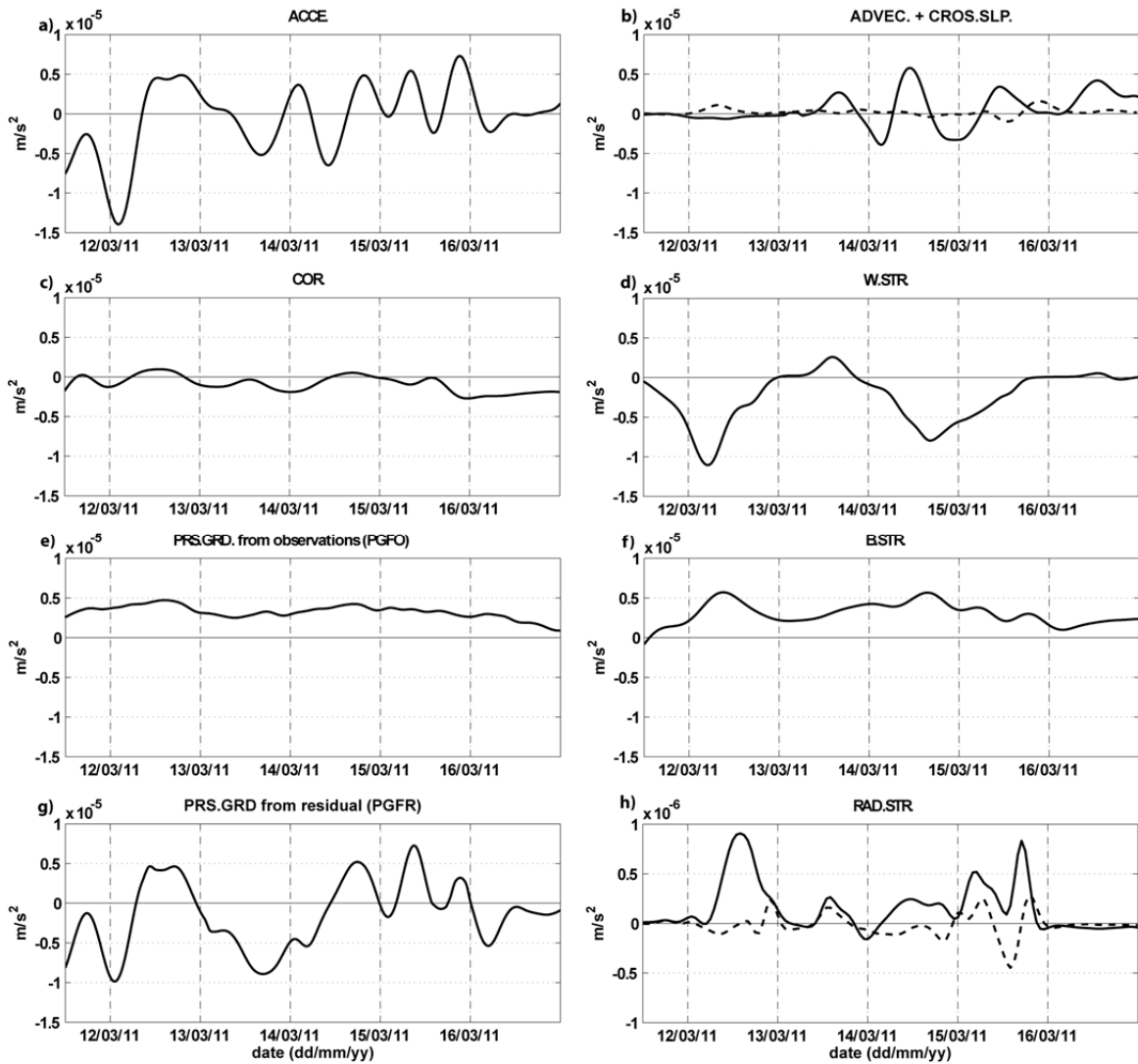


Figure 4. Estimates for the along-shelf momentum terms at 25 m. Left-hand-side terms of Equation 1: (a) acceleration terms (ACCE. $\delta v/\delta t$); (b) advective (solid line, ADVEC $\delta v^2/\delta y + \delta(vu)/\delta x$) and cross-slope (dashed line, CROS.SLP. $(uv/H) \delta H/\delta x$) terms estimated from the currents at the neighboring ADCP locations; (c) Coriolis (COR. $f u$). Right-hand-side terms of Equation [1]: (d) wind stress term (W.STR. $\tau_{ys}/\rho H$); (e) pressure gradient force from observations (PGFO term; $-g \delta \eta/\delta y$); (f) bottom stress term (B.STR. $-\tau_{yb}/\rho H$); (g) pressure gradient force from residual (PGFR); (h) radiation stress term (RAD.ST. $-(1/\rho H) \delta S_{xy}/\delta x$ solid line and $-(1/\rho H) \delta S_{yy}/\delta y$ dashed line). Notice the change in the vertical scale in panel (h). The data used for estimating the momentum terms have been low-pass filtered, with a cut-off frequency of 12 hours. The date indicates 00:00 UTC.

Therefore, this otherwise solid manuscript needs to be upgraded. It stands ‘in between’: it is far from being rejected, but, again, it needs to be upgraded.

Technical corrections

1. Abstract, lines 10-11 and 15-16, statements like:

‘...apparently reflecting the incapacity of the bottom stress to dissipate the high kinetic energy of the system’ and ‘...Estimates of the frictional time and Ekman depth confirm the prevailing frictional response at 24m. are apparently somehow in disagreement: if the (bottom) friction is not sufficient to

dissipate the kinetic energy, then one can hardly say that the response is prevalingly frictional. If both statements are to hold, then appropriate explanation should be given, but not in the abstract.

We refer to “frictional domain” as oppose to “inertial domain”. As depth increases, the frictional terms tend to decrease and the Coriolis term tends to increase as we mention in the discussion. However, some misunderstanding may arise with regard to the “oscillations flows” if we use this simplification. In consequence, we modified the abstract and the discussion clarifying this point (see point mentioned previously): we remove the “prevailing frictional” wording, which did not seem appropriate.

2. Page 900, section ‘Site location and data’

Later in the text authors mention (an important) tidal gauge station at Blanes, a town which is written microscopically on figure 1. Since the pressure gradient term is also calculated with these sea-surface elevation data, this station certainly deserves attention – these are ‘data’ right?

Figure 1 is modified to better mark Blanes tidal-gauge station. We use this station because it was the only point where sea level was recorded during the storm north of the study zone. The data quality was high as the station is periodically maintain by the Technical University of Catalonia staff.

Modification Figure 1

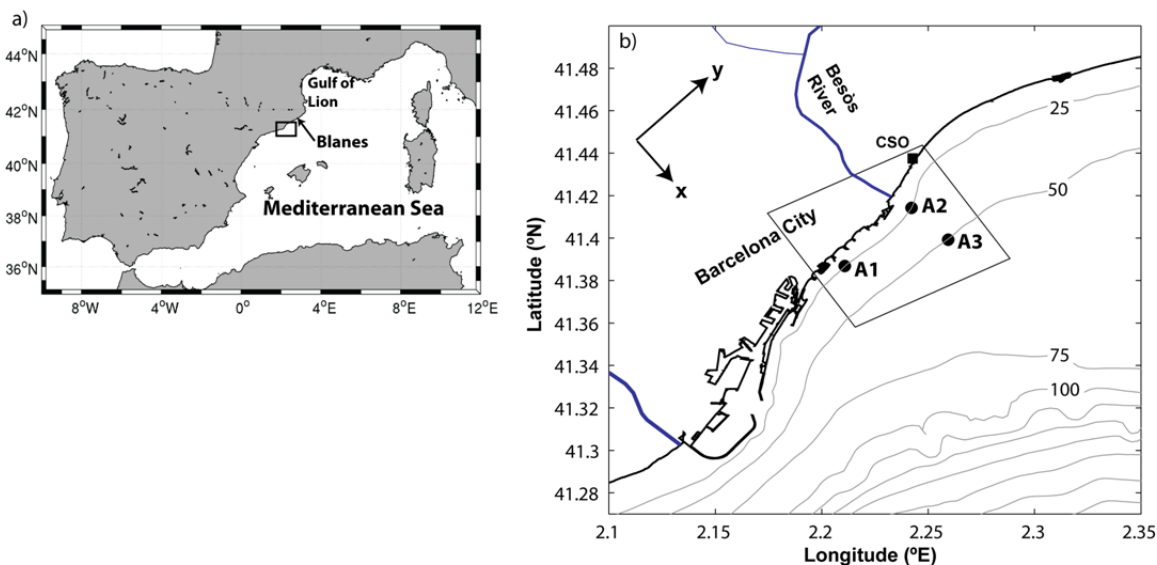


Figure 1. Map of the Western Mediterranean Sea with the study area (panel a). Panel (b) shows the bathymetry of a portion of the Catalan shelf (isobaths every 25 m) with the locations of the ADCP sensors (A1, A2 and A3). A directional wave buoy was placed at A3. The square marker shows the Coastal Station Observatory (CSO) where the wind data were recorded. Panel (b) includes the numerical model domain used to propagate the wave conditions into A2 (black rectangle); the reference system adopted for the momentum balance is also shown.

Authors calculated the pressure gradient terms, which would be impossible to do if those AWAC and RDI instruments were not also equipped with a pressure sensor. The ‘noise level’ of those sensors should be written here and not mentioned later in the text.

A new sentence is included in the text addressing this point in the section 2:

“The ADCP bin size was 1 m and the velocity accuracy was $\pm 0.5 \text{ cm s}^{-1}$ ”

Authors have also used CTD measurements on 17th March 2011 and there is no word about them in this section.

Information about CTD campaigns is included in the manuscript in section 2 “Site location, data and methods” section. Please note that we change the subsection title accordingly to address subsequent comments made by the reviewer.

“In addition, 43 CTD profiles were collected between 17 March and 10 April 2011 in the area surrounding the ADCPs (Grifoll et al., 2012 described the temperature and salinity conditions).”

If authors will improve the manuscript with the shape of the storm field (winds and pressures) then most certainly these synoptic data, together with their elaboration should be entered here.

The synoptic data information is included in the new version of the manuscript in the section suggested by the reviewer (see Figure 2 presented previously).

The paper would be clearer if it would be better structured. This means that this section should also be enlarged with ‘methods’, meaning mostly methods of data elaboration (low pass filtering with a 12 h filter, time and space differentiation), which, according to authors, now deserves attention in the section of ‘results’, which makes this section longer and less readable.

We include the time-series information as the reviewer suggested. We kept the differentiations schemes in the results when we present the momentum terms because it seemed less confusing. The Section 2 title has been modified: “Site location, data and methods”.

Paragraph included in Section 2:

“The time series used for estimating the momentum terms have been low-pass filtered with a $1/12 \text{ h}^{-1}$ cut-off frequency to avoid short-time fluctuations. This choice of filter window is consistent with the velocity spectra that showed limited energy in frequencies higher than inertial ($f^I = 18.15 \text{ h}$; Grifoll et al., 2012).”

Also the description of the numerical model of waves should be here. The horizontal resolution of the wave model should be written here (not on page 905, line 25 under ‘Results’), together with the description of the input wind data, which is missing. Since authors mentioned the wave model, this certainly means that they have available wind (and air-pressure) model data over the observed shelf area.

The information about the numerical wave model (mesh, winds, etc.) has been moved to “Site location, data and methods” in the new version of the manuscript. You are right, it seems more appropriate.

3. Page 901, lines 19-20: ‘The cross-shelf flow (Fig. 2c) was less intense than the along-shelf flow...’ True, but not so much during the times of peak winds. It is hard to deduce values of currents from plots 2 b and 2 c because the color scale is different (-0.4 to 0.4 m/s, or -0.1 to 0.1 m/s), which should be unified.

We made some printing tests. If we unified the color scale the visualization of the cross-shelf flow and its reversals in depth (See Figure R1) was more challenging. So, we keep the original version of the Figure assuming that both presentations have advantages and disadvantages.

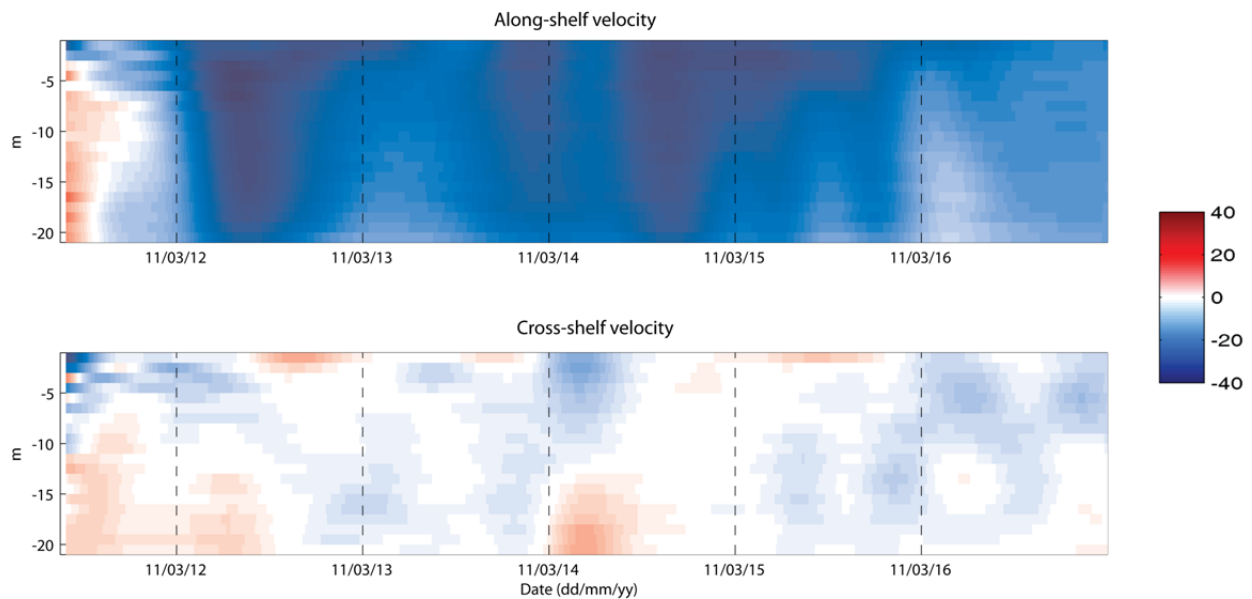


Figure R1. Printing test unifying the scale of the colorbar.

4. Page 901, lines 24-27: ‘The second wind peak (14 March 15:00UTC) was characterized by an intensification of the southeastward flow, while the cross-shelf flow was also enhanced. During the second peak (14 March), the onshore surface flow was compensated by a return flow near the bottom.’ At this point one should be more precise: during the first half of the second storm, when the rise of wind speed (stress) is present, there was an intensification of the cross-shelf flow that was onshore at the surface and offshore near the bottom. An intensification of the southeastward flow over the whole water column (dark blue on figure 2b, seen only when a reader makes a ‘huge zoom on figure 2) looks to be reached a little later, when the wind peak of the second storm occurred. It looks like the along-shelf current follows the (along-shelf) wind stress. After the peak of the second storm, however, when the wind stress decreases with time, there is apparently a reversed situation with regard to the cross-flow: the offshore current at the surface and the onshore one near the bottom. At least this is what this referee could see from those plots b and c on figure 2. The ‘phase delay’ of these (three) processes during the second storm might be important for the explanation of ‘what was going on’.

R2.4. New sentences have been included to describe in detail the oscillations observed in the cross-shelf flow. Also, we highlight in the new version of the manuscript the relation between the cross-shelf oscillations and the oscillations observed in the depth-averaged along-shelf flow (see modifications presented previously in the section 4.1). Obviously the velocity evolution in depth was affected by the presence of transient waves.

Modifications in “Event description” section 3.1 leads a final document like this:

“During the first day of the storm (12 March), the depth-averaged along-shelf current (Figure 3.d) was toward the southwest with a maximum during 12 March 07:00 UTC (two hours after the wind stress peak). During the calm day (13 March 00:00 - 22:00 UTC), the wind changed direction slightly toward the northeast (peaking at 13 March 15:00 UTC), but the along-shelf currents

maintained a similar magnitude and structure than the day before. During the second wind peak the situation repeated itself, but with the along-shelf flow displaying some oscillations.

The cross-shelf currents also displayed a similar time evolution during both wind peaks: the cross-shelf flow intensified with the wind, onshore at the surface and offshore near the bottom; as the wind stress decreased, the flow reversed, turning offshore at the surface and onshore near the bottom (Figure 3.d). During the calm day, the cross-shelf flow was weakly onshore. During the last day of the storm (15 March), the surface wind stress decreased gradually from 0.2 Pa to zero (15 March 23:00 UTC). The along-shelf flow remained to the southwest throughout the water column, and the cross-shelf flow was offshore in the sub-surface layers balanced by onshore currents near bottom.”

5. Page 902, lines 8-9: ‘the depth-averaged current in the along-shelf direction (Fig. 2d) adjustment observed was toward the southwest with a maximum peak during 12 March 07:00UTC’. Here it seems appropriate to add that this happened two hours after the wind-stress peak of the first storm.

Included in the new version of the manuscript (see point addressed previously):

“During the first day of the storm (12 March), the depth-averaged along-shelf current (Figure 3.d) was toward the southwest with a maximum during 12 March 07:00 UTC (two hours after the wind stress peak).”

6. Page 902, lines 11-13: ‘The wave conditions measured at A3 were characterized by two significant wave height peaks (Fig. 3f) from the E–SE direction with a wave period of 8 s.’ It seems important to point out that the peaks of significant wave height followed the peaks of (along-shelf) wind stress with an even larger delay than that of the along-shelf currents, most likely meaning that swell waves play a larger role. Nonetheless, if one again makes a ‘huge zoom’ on the figure one sees that the radiation stress of wind waves has values on an order of magnitude lower than other terms in the equation of motion.

The figure is designed to be in full paper size. However we have modified the figure enlarging the labels. We note the lower order of magnitude of the radiation stress in the figure caption (see Figure 4 shown previously). Figure 4 in the new version of the manuscript is Figure 3 in the old version of the manuscript.

We include this sentence in the “Event description” section:

“The peaks of significant wave height followed the peaks of (along-shelf) wind stress with an even larger delay than that of the along-shelf currents, most likely meaning that swell waves play a larger role.”

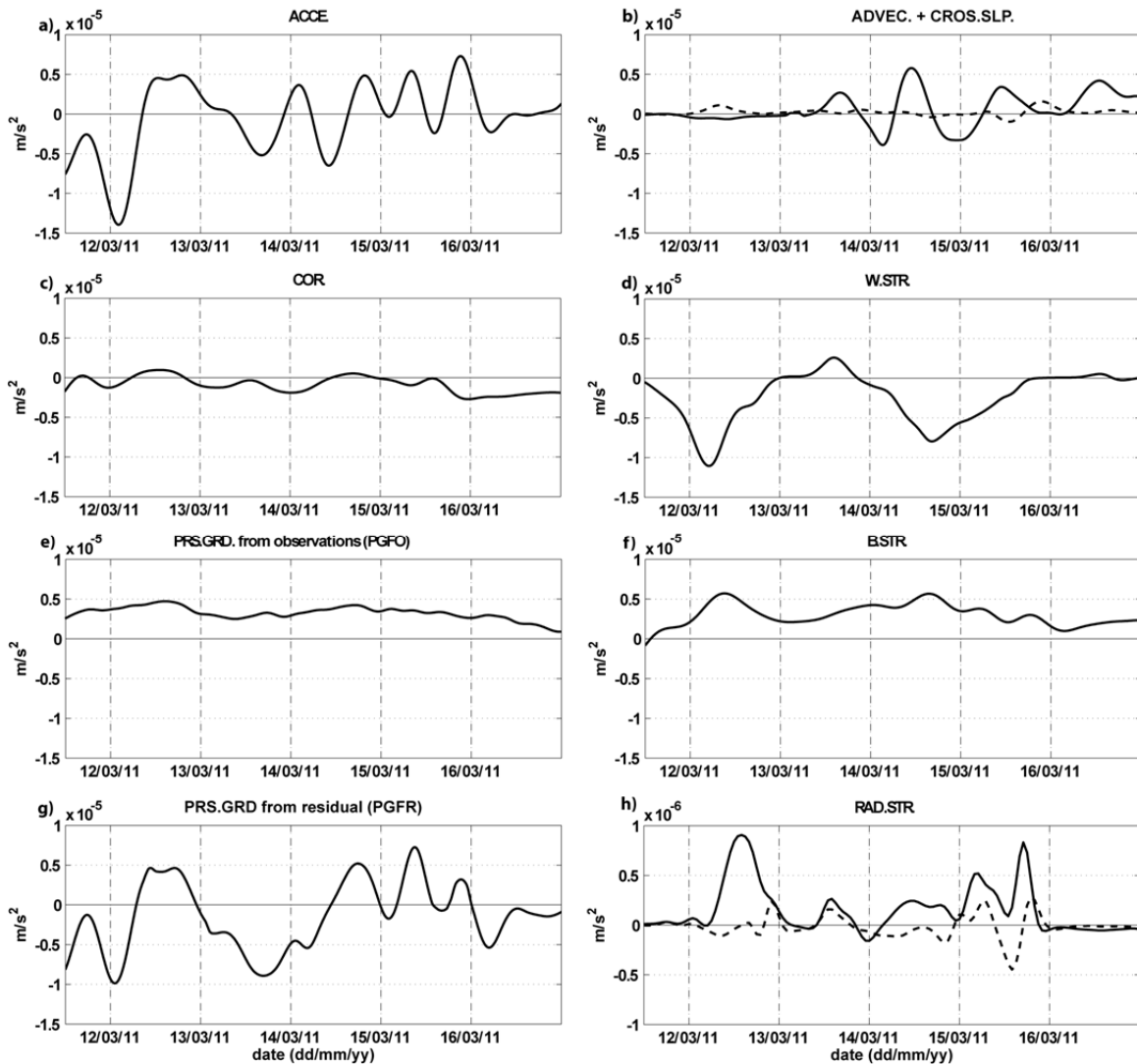


Figure 4. Estimates for the along-shelf momentum terms at 25 m. Left-hand-side terms of Equation 1: (a) acceleration terms (ACCE. $\delta v/\delta t$); (b) advective (solid line, ADVEC $\delta v^2/\delta y + \delta(vu)/\delta x$) and cross-slope (dashed line, CROS.SLP. $(uv/H) \delta H/\delta x$) terms estimated from the currents at the neighboring ADCP locations; (c) Coriolis (COR. $f u$). Right-hand-side terms of Equation [1]: (d) wind stress term (W.STR. $\tau_{ys}/\rho H$); (e) pressure gradient force from observations (PGFO term; $-g \delta \eta/\delta y$); (f) bottom stress term (B.STR. $-\tau_{yb}/\rho H$); (g) pressure gradient force from residual (PGFR); (h) radiation stress term (RAD.ST. $-(1/\rho H) \delta S_{xy}/\delta x$ solid line and $-(1/\rho H) \delta S_{yy}/\delta y$ dashed line). Notice the change in the vertical scale in panel (h). The data used for estimating the momentum terms have been low-pass filtered, with a cut-off frequency of 12 hours. The date indicates 00:00 UTC.

The introduction of the advective terms needs to be done correctly. The depth average of the two advection terms in the along-shelf momentum equation yields at least an additional term like - next to the existing term and a term like - next to the existing term. Both additional terms, not to mention others, hardly seem 'to vanish' by the correct usage of the continuity equation. Terms with the gradient of the depth in the across-shelf sense are likely to have at least the same order of magnitude as those that have been explored. Authors would agree that we may reasonably suppose for the order of magnitude $v = 0.1 \text{ m/s}$, $H = 50 \text{ m}$, $= 25/103$, where the distance between A2 and A3 station is taken as 1 km. This gives $uvH/Hx \approx uvx \approx 2v/H \approx 2 \times 0.1/103 \approx 0.002 \text{ m/s}^2$ which is the order of the local acceleration term and other important terms in the equation (1). Therefore, the analysis of the insignificance of the advection terms in the manuscript looks incomplete.

You are right. In the old version of the manuscript we neglected the mentioned terms. Now, they are included in the analysis. The relevant term is now included in Figure 4 (See previous comment). Also a comment of the estimation of this term is included in the new version of the manuscript as we shown previously. A typo was found in the manuscript (the related distance between A2 and A3 was 2.02 km instead 1 km as we mentioned in the old version of the manuscript). Obviously the right distances were included in the analyses. As a consequence, the new term is smaller than the “pure” advection term, with only sizeable values after the second peak of the storm. The new figure is included in the manuscript and presented in this document.

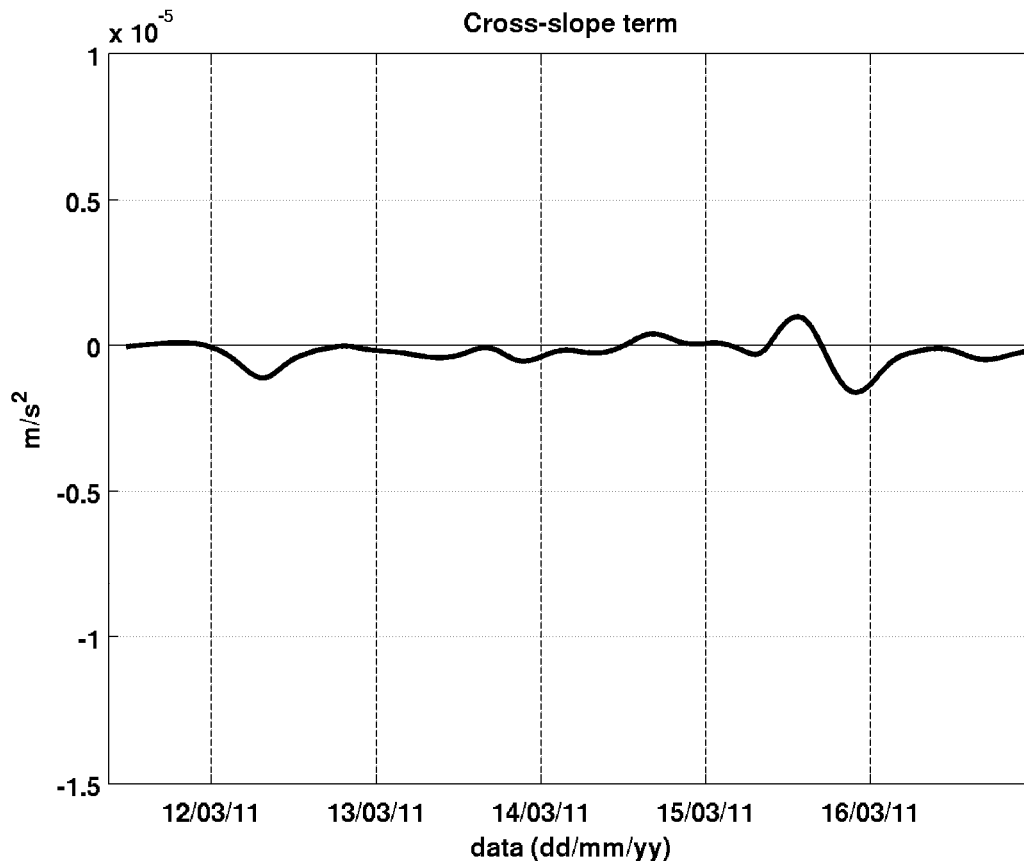


Figure R2. Cross-slope term $(v \cdot u/H) dH/dx$. Note the same scale than for the Momentum Balance manuscript plot was used.

8. Page 903, top two paragraphs and the paragraph around line 25: Although authors made it clear that by using the cut-off filter of 12 h little energy remained in frequencies higher than inertial, it is exactly this frequency, and frequencies ‘slightly above it’, that matter for reasoning about what is going on the Catalan shelf during storms. They wrote: ‘...After the wind direction reversal, the acceleration term oscillates indicating a readjustment of the momentum balance (i.e. a relaxation period that lead to the pre-storm during storm conditions).’ It is true that the relaxation time (meaning friction mechanism) matters. Friction, however, cannot produce oscillations of acceleration before, during and after the second storm. Is there really not a period of 18.15 h seen between the first two minima of the along-shore local acceleration between 13 and 14 March 2011 (figure 3 a)? Could it be that the water mass with inertial oscillation passed over station A3? Between the two consecutive minima of the ‘advection’ terms this period also seems to prevail. There also seem to be oscillations with the time intervals between neighboring minima or maxima that have a higher frequency than inertial. This is

hard to deduce from images by the reader because of the microscopic and unpleasant nature of the plots.

We agree that the friction can not produce these oscillations. According to the previous comments and the manuscript modifications, transient waves in the lee of the storm is considered as a plausible explanation jointly with the coastal trapped wave mechanism (see new version of the section 4.1 in the discussion and modifications in the abstract and conclusions). We also modify the manuscript in ADVEC term analysis. In addition, we modify the plots to enhance their interpretation (see Figure 4 presented previously).

“The non-linear or advection terms are estimated by finite differentiation between the adjacent ADCP measurements (Kirincich and Bart, 2005; Figure 4.b). The velocity advection terms (ADVEC in Equation 1) were small during the first peak of the storm but later oscillated in a manner similar to the acceleration term.”

Anyway, during the calm periods after storms one would expect the long free waves to move around the shelf. Despite the reasonable number of references put down by the authors, one is missing, i.e. the investigation into the possible ‘arrested topographic wave’ (Csanady, JPO, 1978), which follows from linear theory without any advection. This theory states that long waves with periods longer than the inertial one ($1/f$) are confined to a sloping shelf and are not radiated away. Their amplitude decreases exponentially, with an offshore. decaying scale $L_x = [rLy/(fs)]^{0.5}$ (Pettigrew and Murray, 1986. Baroclinic processes on Continental Shelves, Coastal and Estuarine Sciences 3, 95-108), where Ly is the along-shore length scale determined by the wind field, r is the coefficient of linear friction, which was thoroughly determined by authors, f is the Coriolis parameter and s is the bottom slope which hardly enters into the analysis in this manuscript, which seems to be deficient for processes on a sloping shelf. This expression (a similar one is written by Csanady in JPO 1978 in expression (21), where the along-shelf wave number is used instead of Ly) should be easily explored by measurements and is linked to the cross-shelf modulation of long waves. As Brink pointed out (Brink, 1998. the Sea, vol. 10, Wind-driven currents over the continental shelf, 3-20) on page 16 (6.1 Storm surges) storm surges may have frequencies that are higher than inertial. In this case there is an off-shore radiation of long waves that rules out coastal trapping.

Authors should also explore the cross-shore momentum balance, to see if the offshore acceleration (not examined) is present, or that it is not of much importance and there are signs of geostrophic balance, which is typical for trapped shelf waves. They may also verify the apparent ‘in-phase motion along-shelf of topographic coastal wave, if that one is trapped and its amplitude at A3 station is smaller than that at A2 station ($\omega < f$). None of these views is present in the manuscript.

The new version of the manuscript addresses this point discussing the high-frequency motion of the storm surge. A careful analysis of the observations in A2 and A3 does not show a clear radiation of the velocities offshore as the linear theory of coastal trapped waves suggest. Perhaps due to the relatively small distance between A2 and A3 in comparison to the offshore decaying scale (L_x) may explain the differences between the cross-shelf flow between A2 and A3 during and post-storm. The cross-shelf momentum balance shows an evident geostrophic nature but the analysis is limited by data limitations to determine the cross-shelf flow. Please note that the Coriolis terms is larger than the frictional terms $f \cdot v > (\tau_{wind} + \tau_{bottom}) / (\rho \cdot H)$ for 25 and 50 m water depth.

9. Page 905, line 6: the value of $r = 8.5 \times 10^{-4}$ m/s seems to be linked to the first storm and the peak of PGFO during it. What about the PGFO peak during the second storm and consequently the 'representative' value of r for the second storm?

Due to the presence of the transient and coastal-trapped waves it is more difficult to estimate the frictional parameter during the second storm. As we mentioned previously, during the first peak of the storm, we assume that the flow starts from rest, so the response is almost "linear" in terms of acceleration and bottom friction.

10. Page 907, lines 9 and 10: 'The peak in the acceleration term occurs before the wind maximum as a result of the enhanced frictional dissipation and the increase of the pressure gradient force. Thus the along-shelf current is limited by the intensity of the bottom friction'. Authors did not pay attention to 'instrument clocks' in the section of 'data'. Since it is hard to extract the time delay from figure 3 between the wind peak and the acceleration peak (a few hours?) one needs to be certain that the timing of ADCPs matches the hours of the timing of the wind measurements (all in UTC) and that the clock error of the instruments is much smaller than this delay. Currents are not only limited by the bottom friction – they are actually limited by the wind-setup piling of the sea-surface.

The instrument clock errors expected was on the order of seconds. Before the mooring operation, the devices were synchronized computationally to acquire synchronous data. All the times are in UTC (see modifications in the text included previously).

11. Page 907, lines 27-28: 'These fluctuations (during the second peak) likely are a result of the increased energy available in the system, not properly dissipated by the bottom stress.' This is not a good argument. Friction may damp more or less oscillations, but the cause of them is still unclear and should be linked to some known form of motion on sloped shelf areas. Was the dissipation during and after the wind stress peak of the first storm not sufficient to damp the oscillation of the acceleration, while during the second storm it was sufficient? This seems strange.

We have modified the manuscript addressing this point. As we mention previously, the oscillations are due to free waves. The discussion is enhanced by including the transient and coastal trapped wave as a source of the oscillation motion as we mention previously.

12. Page 908, lines 7-10: Authors are not convincing in their explanation of the small advective terms during the first storm (first wind stress peak) while during the second peak the non-linearity of the flow results as a lack of dissipation of kinetic energy. One actually needs to justify why terms like $\frac{\partial u}{\partial x} + \frac{\partial v}{\partial y}$ are much smaller during the first storm and larger during the second storm. If we confine ourselves only to these terms with horizontal gradients of products of depth, averaged velocity components most certainly depend on the extension of the atmospheric structure of both storms that force the coastal shelf sea and also travel over it at a certain speed. The latter matters (with respect to the speed of long waves) if one would try to explore the resonance forcing of long waves. Apart from time series of measurements at one meteorological station we do not have a clue about what these storms above the sea-surface looked like.

We link the oscillation of the advective term with the presence of "free waves". From the measurements it was difficult to estimate the response of the nonlinear terms with the trapped waves, but the shape of the depth-averaged, the acceleration term and the additional wavelet plots included in the new version of the manuscript may indicate some relation between the oscillation in the non-

linear terms and the mentioned time series. This relation is mentioned in the discussion at the end of the section 4.1:

“Our analysis highlights the importance of the initial conditions (whether the system starts from rest or not) and the complexity of the momentum fluctuations during the development of the storm. A comparison of the shifting momentum during both wind peaks shows that the role of the acceleration and advective terms is quite different. During the first peak, the advective terms are relatively small as a result of the linear response of the pressure gradient and bottom stress to the wind forcing. After the first peak, however, the acceleration and advective terms display fluctuations that might reflect the transient waves and propagation of topographic waves. Hence, the along-shelf velocity during the second peak is the cumulative effect of a local response to wind stress combined with the arrival of topographic waves that barely feel the effect of bottom friction.”

13. Page 909, top paragraph about the calculation of r . This explanation of authors is about the time for frictional adjustment, which in the case of linear friction calculates r iteratively from PGFR and from it the frictional time as H/r . The authors offered a method to calculate the frictional time from the time interval between zero and maximum bottom stress. However, this could also be reversed: by knowing the frictional time, one calculates the coefficient of linear friction $r = H/t_14$, where $t_14 = 14$ hours for the adjustment time of the second storm. This point of view also means that the complicated iterative method given for r is a value that is wrong by almost a factor of two...

We assume that the iterative method would be enhanced with additional measurements but the obtained r value matches the bibliography and is supported by the observation analysis (i.e. the adjustment between depth-averaged along-shelf velocity, acceleration and wind stress). We choose the iterative method because the pressure gradient as a response is “coupled” with the bottom friction in shallow seas. For this reason, we believe that the method is suitable. However the manuscript is modified highlighting this point.

Modifications in the section 3.2 (“Momentum balance in the inner-shelf”):

“The estimation of the drag coefficient depends on the water depth and the along-shelf velocity; large fluctuations in the value of r have been found to occur as the prevalent momentum terms change (Lentz et al., 1999). Typical values for water depths of a few tens of meters are between 10^{-3} and 10^{-4} m s^{-1} (e.g. Winant and Beardsley, 1979). In our analysis, the drag coefficient was close to 10^{-3} m s^{-1} , estimated from the momentum balance evolution as explained below. Linear drag formulations are well established for steady-state conditions but might cause misrepresentations during transient conditions (such as during the passage of a storm). We use the linear formulation as a first estimate of the size of the frictional terms, but also consider the potential effect of non-linear friction (Appendix A). The time series for the bottom stress (B.STR.) term (Figure 4.e) had peak values at times of maximum along-shelf flow, almost immediately after the peak wind stress.”

14. Page 909, lines 24-25: ‘...dependence of the flow on bottom dissipation at depths of the order of 24 m during a storm, precluding the appearance of inertial fluctuations independently of the coastal constraints’. Maybe it is so. Still, there are large oscillations of the along-shore local acceleration and there were statements that friction was not sufficient to damp these fluctuations.

This sentence has been modified to be consistent with the previous modifications suggested by the authors.

15. Page 913, line 9: 'The storm had two separate peaks'. No, this concept is wrong. There were *two* consecutive storms and their horizontal gradients of winds and air-pressure could be quite different. Their travelling speed over the shelf might differ significantly as well. All this matters in the explanation of forced motion.

According to the atmospheric PSL plots from ECMWF included in the new version of the manuscript, there was a single storm from a synoptic point of view. However, we assume that there is not a real consensus about the periodicity of wind stress peak to consider one or two consecutive storm in the NW Mediterranean Sea and this point may lead to a complexity beyond the focus of the manuscript.

Technical corrections

Page 899, line 14: '...found the prevalent terms that the size of the momentum terms...' ↔ '...found in the prevalent terms that the size of the momentum terms...'

Modified. Thanks.

Page 900, line 1: '(from hours to few days)' ↔ '(from hours to a few days)'?

Ok, modified in the new version of the manuscript.

Page 904, line 11: if the bin size of ADCP instruments is 1 m, then it is hardly possible that the first cell would measure currents at the height of 1 m above the sea bottom. There is a blanking distance, plus the height of the frame on which the ADCP is mounted.

You are right. The bins above the sea were not considering the echo of the acoustic signal.

Page 919, figure 1: why do these two figures have to be so small? This is really hard to look at. A zoom on figures shows that they have high-enough resolution. There is the name of the town written (Blanes) with letters that are a height of 1 mm? This name is written between the Balearic Islands and the Catalan coastline, it does not give an idea where Blanes is. All letters, including the names of stations, are simply too small and really unpleasant to a reader (and to this referee).

We expected that this figure will cover the full page width in the final edition of the paper. However we have enlarged the names of the geographical location in the Figure 1 and modified the figure with an arrowhead to locate better Blanes city.

New version of the Figure 1:

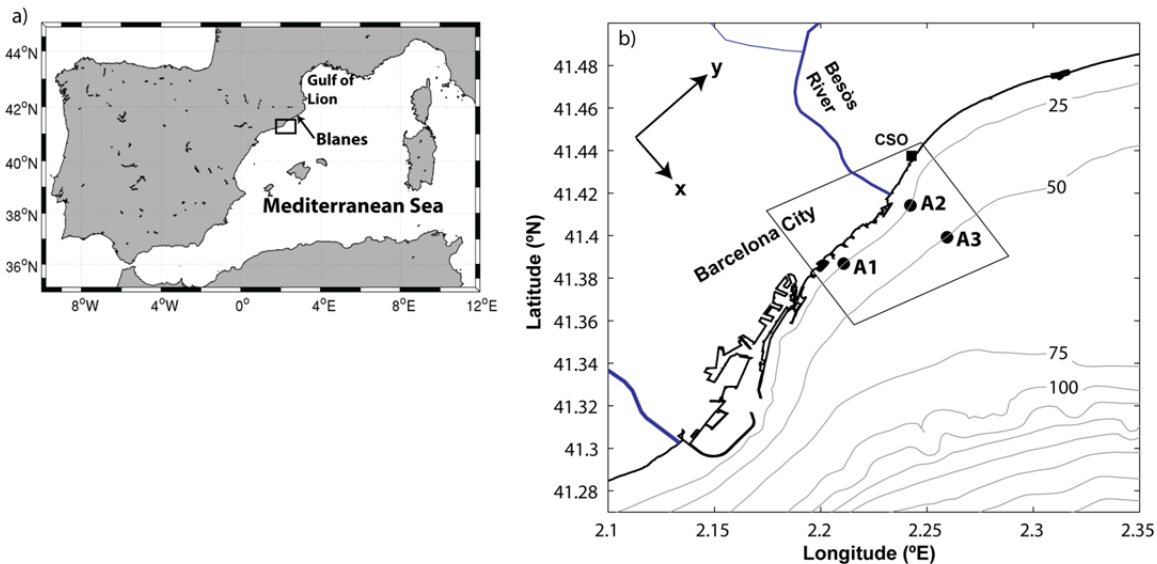


Figure 1. Map of the Western Mediterranean Sea with the study area (panel a). Panel (b) shows the bathymetry of a portion of the Catalan shelf (isobaths every 25 m) with the locations of the ADCP sensors (A1, A2 and A3). A directional wave buoy was placed at A3. The square marker shows the Coastal Station Observatory (CSO) where the wind data were recorded. Panel (b) includes the numerical model domain used to propagate the wave conditions into A2 (black rectangle); the reference system adopted for the momentum balance is also shown.

Pages 920 and 921, figures 2 and 3: while all plots on the figures are again too small and unpleasant, one could see with a huge zoom that while on figure 2 the time scale is labeled in ‘units’ yy/mm/dd (=year/month/day), the time scale on figure 3 is labeled in ‘units’ dd/mm/yy (=day/month/year), which is confusing. While figure 2 has the full day of 11th March on the time scale, figure 3 does not. Labels of plots, like a, b, c,... are missing on both figures. These labels are otherwise written in figure captions of both figures, but they are missing on plots. Figure 2 should have the same color bar scale on plots b and c to have a better feeling about how the cross-shelf velocity is smaller than the along-shelf velocity.

We corrected the typos identified in the figures (see Figures presented previously).

New version of the Figure 3 (Figure 2 in the old version of the manuscript):

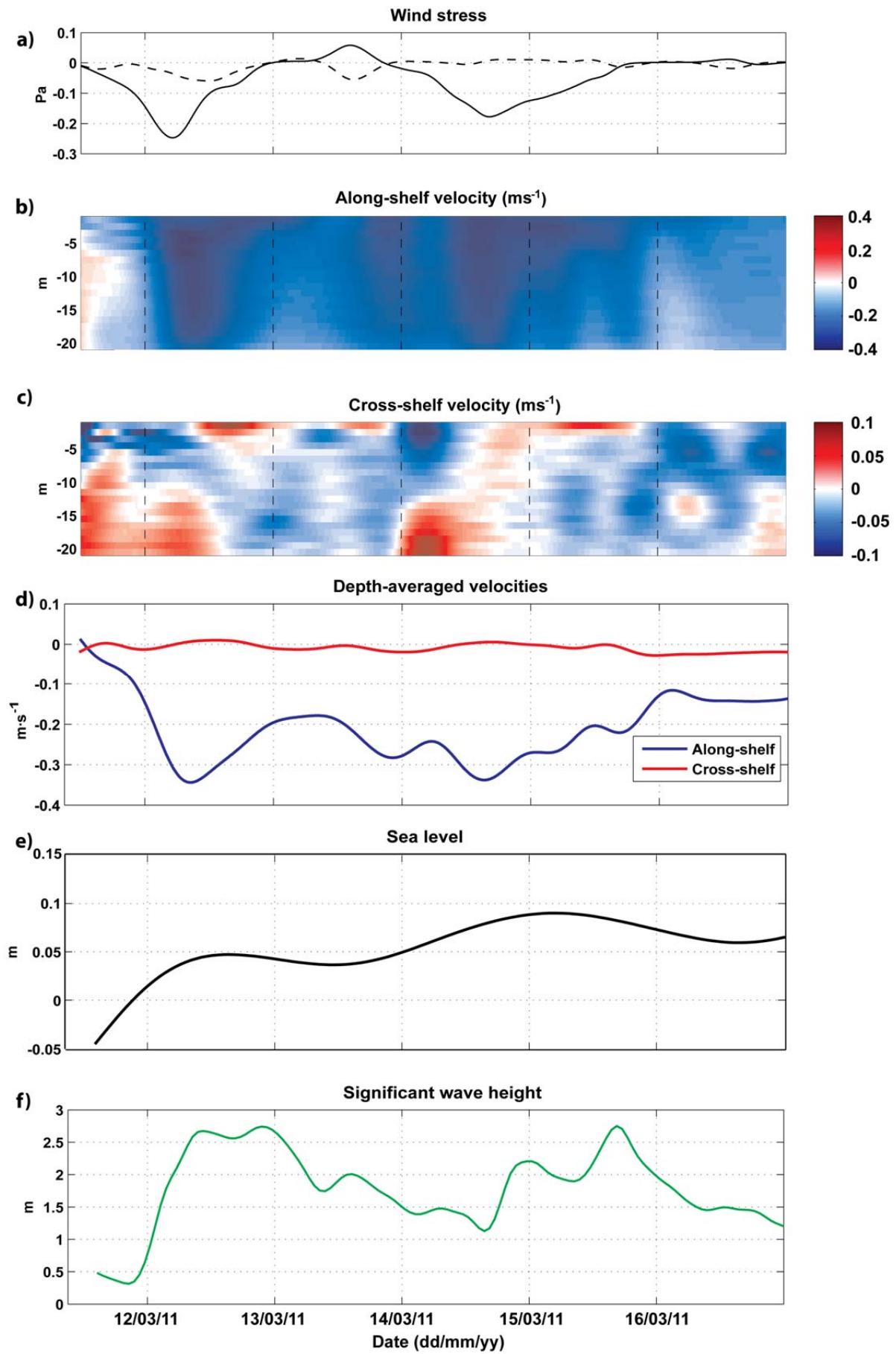


Figure 3. (a) Time series of wind stress measured at the Coastal Observatory Station (the continuous line for the along-shelf wind component and the dashed line for the cross-shelf wind component). (b) Along-shelf velocity. (c) Cross-shelf velocity. (d) Depth-averaged along- and cross-shelf velocities. (e) Detided sea-level variations. (f) Significant wave-height. The velocities and sea level fluctuations were measured at station A2, and the wave conditions at station A3. The date indicates 00:00 UTC.

Page 922, figure 4: too small, letters are too small to read.

Ok. The figure has been resized (Figure 4 is now Figure 5 in the new version of the manuscript):

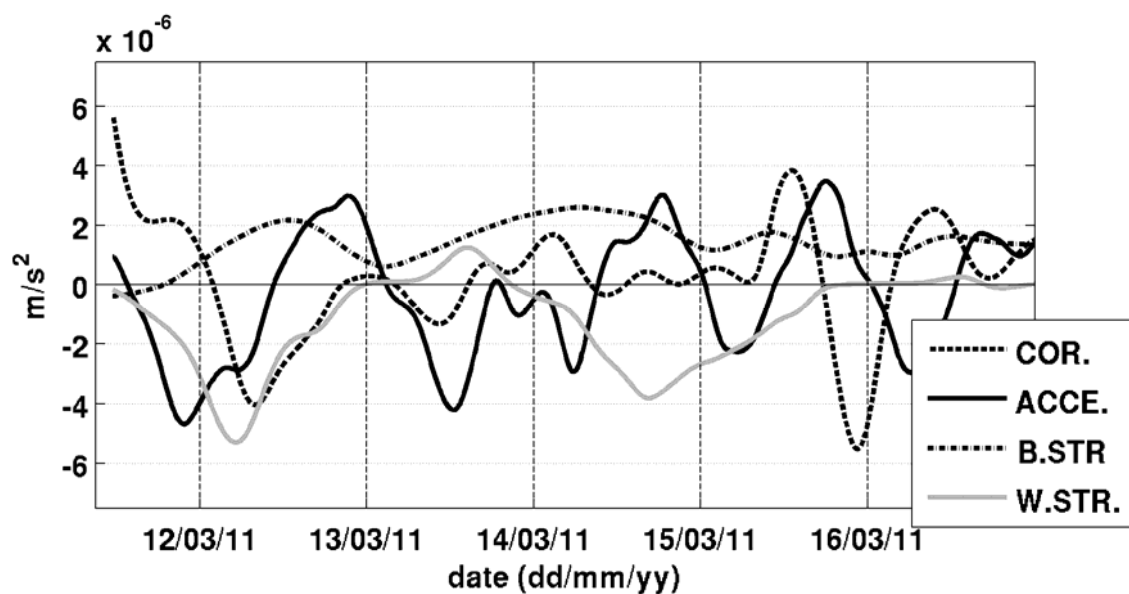


Figure 5. Estimates for the along-shelf momentum terms at 50 m. Left-hand-side terms of Equation 1: Acceleration terms (ACCE. $\delta v/\delta t$) and Coriolis (COR. fu). Right-hand-side terms of Equation [1]: wind stress term (W.STR. $\tau_{ys}/\rho H$) and bottom stress term (B.STR. $-\tau_{yb}/\rho H$). The data used for estimating the momentum terms have been low-pass filtered with a cut-off frequency of 12 h^{-1} . The date indicates 00:00 UTC.

Appendix included in the new version of the manuscript:

“Appendix B: Topographic waves over the continental shelf

Here, we follow Csanady (1982, section 4.5) to estimate the size of the coastal propagating anomalies. We look at the non-forced propagation of a sea surface perturbation, with elevation η , generated at some earlier time in some upstream location along the coast. We keep the same coordinate convention as in the main text, with (x, y) respectively directed cross-shelf and along-shelf (positive offshore and to the northeast). Following Grifoll et al. (2013), we let the dominant terms in the cross-shelf direction to be in geostrophic balance. Hence, the linearized depth-integrated momentum- and mass-conservation equations for non-stratified and frictionless conditions are:

$$\begin{aligned}
-fv &= -g \frac{\partial \eta}{\partial x}, \\
\frac{\partial(vH)}{\partial t} + fuH &= -gH \frac{\partial \eta}{\partial y}, \\
\frac{\partial(uH)}{\partial x} + \frac{\partial(vH)}{\partial y} &= -\frac{\partial \eta}{\partial t}.
\end{aligned} \tag{B1}$$

Let us idealize our coastal ocean as having the water depth independent of the along-shelf distance, $H=H(x)$. Taking the curl of the momentum equations and using the mass-conservation equation leads to the following vorticity equation (constant f condition):

$$\frac{\partial^2(vH)}{\partial t \partial x} - f \frac{\partial \eta}{\partial t} = -g \frac{dH}{dx} \frac{\partial \eta}{\partial y}. \tag{B2}$$

In the cross-shelf direction the change in water depth is much greater than the change in surface elevation (the equivalent of assuming the rigid lid approximation for the mass-conservation equation), i.e. $\partial(vH)/\partial x \gg \partial \eta / \partial t$. Hence, we may safely neglect the second term in the left-hand-side of equation (B2) so that, using the first equation from B1, we get:

$$\frac{\partial^2}{\partial t \partial x} \left(H \frac{\partial \eta}{\partial x} \right) + f \frac{dH}{dx} \frac{\partial \eta}{\partial y} = 0. \tag{B3}$$

We need two boundary conditions to solve this equation. The first one comes from the condition of no-normal flow at the coast; from the second equation in B1, and with the help of the first of these equations, we obtain

$$\frac{\partial^2 \eta}{\partial t \partial x} + f \frac{\partial \eta}{\partial y} = 0, \quad \text{at } x = 0. \tag{B4}$$

The second condition may be simply specified from the requirement of a finite-size perturbation; from the first of equations (B1) this is equivalent to setting that far enough from the coast the elevation of the perturbation tends to zero:

$$H \frac{\partial \eta}{\partial x} = 0, \quad \text{at } x = L_x. \tag{B5}$$

Here, we choose L_x to be the width of the continental shelf (i.e., the offshore extent of the perturbation is limited by the width of the coastal band). For our study, we take this to be the characteristic width of the continental shelf north of Barcelona, or about 40 km.

The solution of equation (B3) subject to the boundary conditions (B4 and (B5) is obtained through separation of variables, $\eta(x, y, t) = \phi(y, t) \chi(x)$. The equation for $\phi(y, t)$ becomes

$$\frac{\partial \phi}{\partial t} - c_i \frac{\partial \phi}{\partial y} = 0, \tag{B6}$$

where c_i is the separating constant. The general solution corresponds to a wave propagating in the negative y direction (in our case, towards the southeast), $\phi(y + c_i t)$, showing that c_i corresponds to the phase speed of the travelling perturbation.

Following Csanady (1982), let the water depth be a linear function of the cross-shelf distance, $H(x) = xH_0/L_x$; the equation for $\chi(x)$ becomes

$$\xi \frac{d^2 \chi}{d\xi^2} + \frac{d\chi}{d\xi} + \chi = 0, \tag{B7}$$

where $\xi \equiv fx/c_i$. The boundary condition at the coast becomes $(c_i/f)d\chi/dx + \chi = 0$, and the condition at $x = L_x$ turns into $d\chi/dx = 0$. Equation (B7) together with these boundary conditions is an eigenvalue problem, with different solutions for a discrete number of positive c_i values. The solution that satisfies the boundary condition at the coast is $\chi = AJ_0(2\xi^{1/2})$

where J_0 is a Bessel function of order 0, and A a constant. The boundary condition at $x = L_x$ sets the possible c_i values, those that satisfy $J_1[2(fl/c_i)^{1/2}] = 0$, where J_1 is a Bessel function of order 1. The faster wave corresponds to $c_1 = fL_x/3.67$, having the simplest structure: maximum velocity at the coast that decreases to zero at L_x .

From the first of equations (B1), the along-shelf velocity is $v = -(gA\phi)/(c_i f x)^{1/2} J_1(2\sqrt{i})$. The maximum velocity takes place at the coast, given by $v = -(gA\phi)/c_1 = -(3.67 gA\phi)/(fL_x)$, its magnitude depending on the elevation $A\phi$ at the coast. In Figure 3e, we see changes in elevation as large as 0.05 m taking place on time scales of about 1.5 days, which would represent velocities of about 0.5 m s^{-1} , which is in fair agreement with the observed oscillations (Fig. 2b).

The periodicity of these perturbations depends on the size of the region where they are generated, which sets the along-shelf wavenumber $k = 2\pi/L_y$. The shortest period corresponds to the fastest propagating perturbations, which are also the ones that result in the largest along-shelf velocities; it turns out to be $T \equiv 2\pi/\omega \equiv 2\pi/(c_1 k) = (3.67/f)(L_y/L_x)$. If we choose L_y to be 120 km, or about the size of the domain with maximum gradients in sea-level pressure (and hence maximum winds) (Figure 2), we get $L_y/L_x \cong 3$ and the period is about 32 hours. This number is to be taken only as a very rough estimate but yet it suggest that some of the energy in the wavelet and spectra analyses (Figure 6), in the 1-2 day band, comes from propagating topographic waves.”

New references included:

Csanady, G. T.: Circulation in the coastal ocean. D. Reidel Publishing Company, 279 pp., Dordrecht, Holland, 1982.

Gill, A. E.: Atmosphere-ocean dynamics, Academic Press, London, England, 662 pp., 1982.

Jordi, A., Orfila, A., Basterretxea, G. and Tintoré, J.: Coastal trapped waves in the northwestern Mediterranean, Cont. Shelf. Res., 25, 185-196, 2005.

Kundu, P. K., Chao, S. and McCreary, J.P.: Transient coastal currents and inertia-gravity waves, Deep-Sea Res., 30, 10A, 1059-1082, 1983.

Kundu, P. K. and Thomson, J.P.: Inertial oscillations due to a moving front, J. Phys. Oceanogr., 15: 1076-1084, 1985.

Tintoré, J., Wang, D.-P., García, E. and Viúdez, A.: Near-Inertial Motion in the coastal ocean, J. Mar. Syst., 6, 301-312, 1995.